Check for updates

ASME Journal of Computing and Information Science in Engineering
Online journal at:
https://asmedigitalcollection.asme.org/computingengineering

Dynamic Sensor Selection for Efficient Monitoring of Coupled Multidisciplinary Systems

Negar Asadi
College of Engineering,
Northeastern University,
Boston, MA 02115
e-mail: asadi.n@northeastern.edu

Seyede Fatemeh Ghoreishi[1]
College of Engineering and Khoury College of Computer Sciences,
Northeastern University,
Boston, MA 02115
e-mail: f.ghoreishi@northeastern.edu

Coupled multidisciplinary systems involve different disciplines/subsystems with feedback-coupled interactions, illustrating the complex interdependencies inherent in real-world engineering systems. Effective monitoring of a coupled multidisciplinary system is crucial for real-time assessment of the interactions between various disciplines within the system. This monitoring provides the data necessary for detecting and addressing issues in a timely manner and facilitates adaptive decision-making for taking reliable design or control actions. However, processing and analyzing data in real time is computationally intensive, and limited resources, such as computational power, sensor capabilities, and budget, may constrain the extent to which a system can be monitored comprehensively. To address this, this article develops a particle-based approach that dynamically selects a subset of sensors that provides the highest information about the state of the system in real time. The proposed approach first predicts the amount of uncertainty in the estimation of the state of the system given noisy measurements from different subsets of available sensors. Then, it selects the sensors that reduce this uncertainty the most, enhancing the precision and efficiency of the monitoring process. The efficacy of the proposed framework is demonstrated via two coupled multidisciplinary systems in the numerical experiments.
[DOI: 10.1115/1.4065607]

Keywords: coupled multidisciplinary systems, monitoring, dynamic sensor selection, state estimation, multidisciplinary optimization

1 Introduction

Many real-world systems consist of several disciplines interacting with each other dynamically and typically with a great deal of uncertainty associated with each discipline. The interactions between disciplines can be feedforward coupled (unidirectional), in which the output of the upstream discipline becomes the input to the downstream discipline, or feedback coupled (bidirectional), in which the output from one discipline is the input to the other discipline and vice versa. The integration of disciplines and the interactions between them play a key role in the overall behavior of coupled multidisciplinary systems. These systems are common in many applications such as in aerospace and cyber-physical systems [1–9], fluid-thermal–structural modeling and analysis of hypersonic structures [10,11], turbine engine cycle analysis [12–15], satellite performance analysis [16,17], topology optimization [18–20], and more.

The complex nature of coupled multidisciplinary systems, characterized by feedback-coupled interactions, uncertainties, and dynamic behaviors, necessitates monitoring for proactive assessment, optimization, and the continuous improvement of system performance and reliability. The need for effective monitoring of these systems is highlighted by its pivotal role in providing valuable insights into the dynamic interplay between disciplines, offering a comprehensive understanding of the system's behavior. The information obtained from such monitoring facilitates a deeper comprehension of the complex relationships within the system, which is critical for the early detection of anomalies, deviations, and faults, thereby enabling preemptive intervention. This insight plays a crucial role in conducting reliable control strategies and informing the design of these complex, interconnected engineering systems, ensuring their adaptability, resilience, and optimal performance in dynamic and uncertain operational environments. However, challenges arise in balancing the trade-off between comprehensive monitoring and resource constraints, emphasizing the need for innovative approaches and technologies to overcome these complexities and enhance the effectiveness of monitoring in coupled multidisciplinary systems.

Coupled multidisciplinary systems are often partially observable through sensors that provide noisy measurements from different parts of the system with different levels of uncertainty. While all these sensors provide information about the system and collecting all these data could highly benefit the monitoring of coupled multidisciplinary systems, the limits on computational and/or economic resources prevent the analysis of a large amount of data collected from a large number of sensors for real-time monitoring of the system. Processing and analyzing this diverse and often high-dimensional data in real time is computationally intensive, and delays in data acquisition or processing can impact the system's responsiveness. Therefore, there is a need to select the optimal

[1]Corresponding author.

Manuscript received January 21, 2024; final manuscript received May 17, 2024; published online June 7, 2024. Assoc. Editor: Guang Lin.

Copyright © 2024 by ASME; reuse license CC-BY 4.0

Downloaded from http://asmedigitalcollection.asme.org/computingengineering/article-pdf/24/9/091001/7347527/jcise_24_9_091001.pdf by guest on 07 September 2024

subset of sensors in real time that provides the highest information about the system by taking all sources of uncertainty into account. This requires dynamic sensor selection, where the goal is to maximize the accuracy and efficiency of the system monitoring while minimizing the cost and power consumption.

The sensor subset selection problem can be broadly categorized into two main categories developed for static and dynamic systems. In static systems, where the underlying conditions are time independent, the focus is on optimizing the placement and configuration of sensors to capture essential information about the system state. Classical methods for sensor subset selection in static systems include greedy algorithms which iteratively select sensors to maximize information gain or reduce uncertainty [21–24], information theory-based methods utilizing metrics like mutual information and entropy [25–27], optimization techniques aiming to maximize system performance subject to constraints [28–31], heuristic approaches employing intuitive strategies such as thresholding or random selection [32,33], and statistical methods modeling sensor–system relationships through regression analysis or principal component analysis [34,35].

Sensor selection in dynamic systems presents additional challenges due to their time-varying nature, requiring adaptation of selection to changing conditions to capture systems' transient behavior. Several methods have been developed for sensor scheduling in dynamical systems [36–39]. Classical approaches such as those based on Kalman filtering aim to minimize error covariance and optimize sensor placement for linear dynamic systems [40,41]. Extensions of these techniques to nonlinear systems include methods like extended and unscented Kalman filtering, which provide robust estimation in the presence of nonlinearities [42–44]. These methodologies are primarily applicable to systems that can be linearized, and the stochasticity in state and measurement can be represented by Gaussian noise.

The complex and nonlinear dynamics of coupled multidisciplinary systems with nondifferentiable state and measurement processes and non-Gaussian noises hinder the applicability of existing sensor selection methods. More specifically, the uncertainty inherent in both system states and sensor measurements introduces complexity into the selection process. Also, the need for real-time operation in dynamical multidisciplinary systems necessitates selection methods that are computationally efficient and capable of operating in real time. Addressing these limitations requires the development of advanced sensor selection techniques that can adapt to the complexities of dynamical multidisciplinary systems while accounting for uncertainty, resource constraints, and real-time operation.

In this article, we consider the problem of dynamically selecting an informative subset of sensors for collecting measurement data in coupled multidisciplinary systems to estimate the state of the system in real time. To achieve this, we present a general nonlinear hidden Markov model (HMM) representation of coupled multidisciplinary systems, accounting for different sources of uncertainty in the system's state transition and sensor measurement noises. Given this representation, we develop a particle-based sensor selection approach that minimizes the predicted expected uncertainty of state estimation in a Bayesian filtering framework. The proposed framework quantifies the expected posterior uncertainty in a particle-based approach, measured by conditional entropy, and chooses the next subset of sensors in a sequential fashion. The key contributions of the proposed framework, differentiating it from existing methods, are its applicability to a general class of hidden Markov models with nonlinearity of processes and non-Gaussianity of noise characteristics, and offering generalizable monitoring solutions for a wide range of arbitrary objectives that can be expressed through the posterior distribution of states. These features make the proposed method suitable for adaptable monitoring in complex multidisciplinary systems.

This article is organized as follows. In Sec. 2, a detailed description of the proposed framework, including a description of coupled multidisciplinary systems, HMM representation of coupled multidisciplinary systems, dynamic sensor selection, and the proposed particle-based sensor selection approach, is provided. This is followed by Sec. 3, which presents the numerical experiments demonstrating the performance of the proposed framework applied to a coupled aerodynamics–structures system and a coupled heart dipole problem. Finally, Sec. 4 contains the concluding remarks.

2 Proposed Framework

2.1 Coupled Multidisciplinary Systems. A coupled multidisciplinary system consists of a set of interconnected disciplines that interact with each other. The interaction between the disciplines depends on the direction of information flow; this interaction can be feedforward (unidirectional) coupling or feedback (bidirectional) coupling. A feedback-coupled multidisciplinary system with d disciplines interacting with each other dynamically at each time k can be represented as follows [45]:

$$\mathbf{c}_{ij}(k) = f_i\big(\mathbf{c}_{ji}(k-1), \mathbf{u}_i(k-1)\big) + \mathbf{v}_i(k) \tag{1}$$

for $i, j = 1, \ldots, d;\ i \neq j$, where $\mathbf{c}_{ij}(\cdot)$ is the vector of coupling variables output from discipline i and input to discipline j and $\mathbf{u}_i(\cdot)$ is the vector of inputs to discipline i other than the coupling variables, where these inputs are either independent or shared between different disciplines. $f_i(\cdot)$ is the function associated with discipline i, and $\mathbf{v}_i(\cdot)$ is the uncertainty accounting for unmodeled parts of discipline i. An example of a coupled multidisciplinary system with d disciplines is presented in Fig. 1.

2.2 Hidden Markov Model Representation of Coupled Multidisciplinary Systems. In multidisciplinary systems, the coupling variables are the variables that are shared among multiple disciplines, indicating the disciplines' internal behavior, affecting other disciplines' behavior as they get fed into other disciplines, and overall affecting the behavior of the whole system over time as a result of all couplings. Therefore, coupling variables are parts of the system that determine the interactions between disciplines and provide insights into the system-level behavior. In coupled multidisciplinary systems, precisely estimating the values of coupling variables at each time is crucial in order to achieve effective control, design, and analysis of the system. In fact, estimating the correct state of the coupling variables allows one to have accurate knowledge about the current state of the multidisciplinary system as a whole and, consequently, to make informed decisions when choosing control or design inputs to the system or disciplines. Having the functional model of coupled multidisciplinary systems in Eq. (1), we present a general nonlinear/non-Gaussian HMM representation of coupled multidisciplinary systems, consisting of the state and measurement models described below.

State and Measurement Models: Let $\mathbf{x}_k \in \mathbb{X}$ represent the state vector of the system at time-step k ($k = 1, 2, \cdots$), containing all coupling variables of the multidisciplinary system, defined as follows:

$$\mathbf{x}_k = \{\mathbf{c}_{ij}(k) \mid i, j = 1, \ldots, d;\ i \neq j\} \tag{2}$$

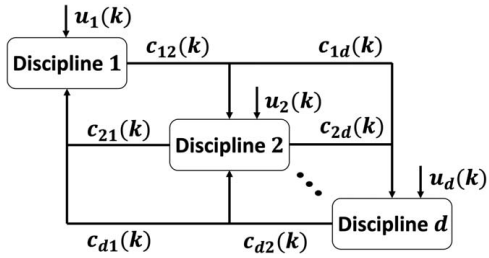

Fig. 1 An example of a coupled multidisciplinary system with d disciplines. $u_i(k)$ and $c_{ij}(k)$ represent inputs and coupling variables at time k, for $i, j = 1, \ldots, d;\ i \neq j$.

Downloaded from http://asmedigitalcollection.asme.org/computingengineering/article-pdf/24/9/091001/7347527/jcise_24_9_091001.pdf by guest on 07 September 2024

and $\mathbf{u}_k \in \mathbb{U}$ be the vector of inputs to all disciplines, excluding the coupling variables:

$$\mathbf{u}_k = \{\mathbf{u}_i(k) \mid i = 1, \ldots, d\} \tag{3}$$

We define $\mathbf{f}(\cdot)$ as the vector containing all discipline functions:

$$\mathbf{f} = \{f_i \mid i = 1, \ldots, d\} \tag{4}$$

which is possibly nonlinear and time-varying, describing the evolution of the state in the system dynamics. In multidisciplinary systems, the coupling variables are often not directly observable, but some noisy and/or partial observations of the states are often available, acquired via sensors. Having these definitions, we consider the following nonlinear HMM describing the state and measurement models:

$$\begin{aligned} \mathbf{x}_k &= \mathbf{f}(\mathbf{x}_{k-1}, \mathbf{u}_{k-1}, \mathbf{v}_k) \quad \text{(state model)} \\ \mathbf{z}_k &= \mathbf{h}(\mathbf{x}_k, \mathbf{s}_{k-1}, \mathbf{w}_k) \quad \text{(measurement model)} \end{aligned} \tag{5}$$

where $\mathbf{v}_k$ is the state noise at time-step k with the probability distribution of $p_{\mathbf{v}}$ (i.e., $\mathbf{v}_k \sim p_{\mathbf{v}}$) containing the unmodeled parts of the system dynamics, $\mathbf{s}_{k-1}$ represents the subset of sensors selected at time-step $k-1$ for monitoring the system at time-step k, $\mathbf{w}_k$ from the probability distribution of $p_{\mathbf{w}}$ (i.e., $\mathbf{w}_k \sim p_{\mathbf{w}}$) represents the measurement noise due to sensor imprecisions, $\mathbf{z}_k \in \mathbb{Z}$ is a vector of noisy measurements observed from the selected sensors, and $\mathbf{h}(\cdot)$ is a function mapping the states to the measurements, for $k = 1, 2, \ldots$. The observed measurements are a nonlinear, noisy, and imperfect realization of the true underlying state of the system, making the measurements random variables, where multiple states are likely to generate the same observation or a single state might generate different observations over time due to noise or variability in the measurement process. The relationships between the states and the measurements are governed by the characteristics of the sensors, which might be apriori known or learned from training data. The state and measurement noises $\mathbf{v}_k$ and $\mathbf{w}_k$ are assumed to be white in the sense that the noises at distinct time points are independent random variables (i.e., $\mathbf{v}_k$ and $\mathbf{v}_l$, and similarly $\mathbf{w}_k$ and $\mathbf{w}_l$, are independent for $k \neq l$). It is also assumed that the noise processes are independent of each other and from the initial state $\mathbf{x}_0$; their distribution is otherwise arbitrary. Without loss of generality, we drop the inputs to the disciplines, i.e., $\mathbf{u}$, in the remainder of the article. However, any control policy can be considered in the proposed method to execute the input $\mathbf{u}$ to the system.

It should be noted that variations in the type and the number of sensors employed to monitor the system lead to differences in the size of the measurement vector, which may be smaller or larger than the size of the state vector. In real-world large multidisciplinary systems, the limitation of resources, including computational power, energy, and budget, imposes restrictions on the feasibility of comprehensive monitoring. Thus, the strategic identification of a subset of sensors becomes not only a necessity dictated by resource constraints but also a means to enhance the efficiency and effectiveness of the monitoring process. In the following subsection, we describe our proposed approach designed to address this imperative by systematically selecting an optimized subset of sensors to monitor a coupled multidisciplinary system.

2.3 Dynamic Sensor Selection. Real-world complex systems need to be monitored properly for timely detection and reaction to possible changes in the system or for prescribing an appropriate intervention for a particular control or design goal. However, the monitoring process is often resource intensive, time consuming, and costly, as it requires a large number of sensors and a large amount of computing power for processing sensor measurements in real time. Hence, to alleviate this computational burden, we propose a framework to select a small subset of sensors to monitor a coupled multidisciplinary system at any given time.

Let $\mathbf{s}_{k-1} = \{i_1, \ldots, i_m\}$ be the indexes of m sensors from which measurements will be collected at time-step $k-1$, where $m \leq N_s$ and N_s indicates the total number of sensors in the system. As indicated in the subscript of $\mathbf{s}_{k-1}$, the sensors should be selected at time-step $k-1$ for monitoring the system at time-step k, resulting in measurements $\mathbf{z}_k$. Let $\mathbf{s}_{0:k-1} = (\mathbf{s}_0, \ldots, \mathbf{s}_{k-1})$ be the selected monitoring sensors at time-steps 0 to $k-1$ with the associated measurements $\mathbf{z}_{1:k} = (\mathbf{z}_1, \ldots \mathbf{z}_k)$ between time-steps 1 to k. The monitoring problem consists of estimating the state (i.e., coupling variables) of the system at each time-step k given the selected sensors and the corresponding measurements $\{\mathbf{s}_{0:k-1}, \mathbf{z}_{1:k}\}$. The goal here is to sequentially select a set of sensors whose measurements provide the highest information about the system, resulting in state estimation with the highest certainty. Toward this, we use entropy as a measure of uncertainty in the posterior distribution of the state at each time. Let $\mathbb{H}$ denote the entropy, which is aimed to be minimized. Therefore, the optimal sensor selection can be obtained as follows:

$$\mathbf{s}_k^* = \underset{\mathbf{s} \in \mathbb{S}}{\operatorname{argmin}}\, \mathbb{H}\big(p(\mathbf{x}_{k+1} \mid \mathbf{s}_k = \mathbf{s}, \mathbf{z}_{k+1}, \mathbf{s}_{0:k-1}, \mathbf{z}_{1:k})\big) \tag{6}$$

where $\mathbb{S}$ is the set of all combinations of available sensors. However, the observation $\mathbf{z}_{k+1}$ associated with each subset of sensors is unknown. In the following subsection, we develop a particle-based approach integrating the Bayesian optimal filtering and the Monte Carlo sampling that takes into account the state and measurement models presented in Eq. (5) and all sources of uncertainty for finding the solution to the sensor selection problem in (6).

2.4 Proposed Particle-Based Sensor Selection Approach. Let $\{\mathbf{x}_k^i, \omega_k^i\}_{i=1}^N$ be N particles and their associated weights at time-step k, where the weights are normalized and thus sum up to one. This set of particles and weights represent the posterior distribution of the state at time k given the selected sensors and the corresponding measurements $\{\mathbf{s}_{0:k-1}, \mathbf{z}_{1:k}\}$ up to this time, as follows:

$$p(\mathbf{x}_k \mid \mathbf{s}_{0:k-1}, \mathbf{z}_{1:k}) \approx \sum_{i=1}^{N} \omega_k^i\, \delta(\mathbf{x}_k - \mathbf{x}_k^i) \tag{7}$$

where $\delta(\cdot)$ denotes the Dirac delta function.

By using the current information, we aim to predict the uncertainty contained in the estimated state at time $k+1$ upon observing any subset of sensors. To achieve this, given $\{\mathbf{x}_k^i, \omega_k^i\}_{i=1}^N$, we first pass the N particles through the state process presented in Eq. (5) to obtain $\{\mathbf{x}_{k+1}^i, \omega_k^i\}_{i=1}^N$ which predict $p(\mathbf{x}_{k+1} \mid \mathbf{s}_{0:k-1}, \mathbf{z}_{1:k})$. For an arbitrary subset of sensors $\mathbf{s} \in \mathbb{S}$, the predicted state particles $\{\mathbf{x}_{k+1}^i\}_{i=1}^N$ are then used to generate N observation particles $\{\mathbf{z}_{k+1}^i\}_{i=1}^N$ associated with $\mathbf{s}$ according to the measurement process in Eq. (5). These observation particles represent $p(\mathbf{z}_{k+1} \mid \mathbf{s}_k = \mathbf{s}, \mathbf{s}_{0:k-1}, \mathbf{z}_{1:k})$, which is the probability distribution of the sensor measurements at time $k+1$ given all previously selected sensors and their corresponding measurements as well as the hypothetically selected subset of sensors $\mathbf{s}$ at this time. Given the predicted observation particles $\{\mathbf{z}_{k+1}^i\}_{i=1}^N$, the probability of the predicted state particles at time-step $k+1$ using the Bayes' theorem can be updated to:

$$\begin{aligned} &p\big(\mathbf{x}_{k+1}^i \mid \mathbf{s}_k = \mathbf{s},\ \mathbf{z}_{k+1}^i, \mathbf{s}_{0:k-1}, \mathbf{z}_{1:k}\big) \\ &= \frac{p(\mathbf{x}_{k+1}^i, \mathbf{z}_{k+1}^i \mid \mathbf{s}_k = \mathbf{s},\ \mathbf{s}_{0:k-1}, \mathbf{z}_{1:k})}{p(\mathbf{z}_{k+1}^i \mid \mathbf{s}_k = \mathbf{s},\ \mathbf{s}_{0:k-1}, \mathbf{z}_{1:k})} \\ &= \frac{p(\mathbf{z}_{k+1}^i \mid \mathbf{x}_{k+1}^i, \mathbf{s}_k = \mathbf{s})\, p(\mathbf{x}_{k+1}^i \mid \mathbf{s}_{0:k-1}, \mathbf{z}_{1:k})}{p(\mathbf{z}_{k+1}^i \mid \mathbf{s}_k = \mathbf{s},\ \mathbf{s}_{0:k-1}, \mathbf{z}_{1:k})} \end{aligned} \tag{8}$$

for $i = 1, \ldots, N$, where $p(\mathbf{x}_{k+1}^i \mid \mathbf{s}_{0:k-1}, \mathbf{z}_{1:k}) = \omega_k^i$. The denominator in Eq. (8) is a normalizing constant ensuring that the posterior

Downloaded from http://asmedigitalcollection.asme.org/computingengineering/article-pdf/24/9/091001/7347527/jcise_24_9_091001.pdf by guest on 07 September 2024

distribution is a valid probability distribution and can be computed as follows:

$$p(\mathbf{z}^i_{k+1} \mid \mathbf{s}_k = \mathbf{s}, \mathbf{s}_{0:k-1}, \mathbf{z}_{1:k}) = \sum_{j=1}^{N} p(\mathbf{z}^i_{k+1} \mid \mathbf{x}^j_{k+1}, \mathbf{s}_k = \mathbf{s})\, p(\mathbf{x}^j_{k+1} \mid \mathbf{s}_{0:k-1}, \mathbf{z}_{1:k}) \tag{9}$$

Finally, the probability of the predicted state particles at time-step $k+1$ given the selected sensors and the associated measurements up to time k and an arbitrary subset of sensors $\mathbf{s}$ and the corresponding predicted measurement particles at time $k+1$, according to the recursive Bayesian state estimation in (8), can be derived as follows:

$$p(\mathbf{x}^i_{k+1} \mid \mathbf{s}_k = \mathbf{s}, \mathbf{z}^i_{k+1}, \mathbf{s}_{0:k-1}, \mathbf{z}_{1:k}) \propto p(\mathbf{z}^i_{k+1} \mid \mathbf{x}^i_{k+1}, \mathbf{s}_k = \mathbf{s})\, \omega^i_k \tag{10}$$

where the likelihood $p(\mathbf{z}^i_{k+1} \mid \mathbf{x}^i_{k+1}, \mathbf{s}_k = \mathbf{s})$ representing the conditional probability of the predicted observation particle given the selected subset of sensors and the predicted state particle can be obtained according to the measurement model in Eq. (5) and the known statistics of the measurement noises for the selected subset of sensors $\mathbf{s}$. Thus, the unnormalized weight associated with each particle $\mathbf{x}^i_{k+1}$ can be calculated as follows:

$$\tilde{\omega}^i_{k+1} \propto p(\mathbf{z}^i_{k+1} \mid \mathbf{x}^i_{k+1}, \mathbf{s}_k = \mathbf{s})\, \omega^i_k \tag{11}$$

and the normalized weights are as follows:

$$\omega^i_{k+1} = \frac{\tilde{\omega}^i_{k+1}}{\sum_{j=1}^{N} \tilde{\omega}^j_{k+1}} \tag{12}$$

As outlined in Eq. (6), the goal is to select the subset of sensors that contribute the most in reducing the uncertainty, i.e., entropy, of the estimated state at each time. Therefore, after obtaining the predicted state particles and the associated weights, we need to compute the predicted entropy for the state distribution at time $k+1$ given the selected subset of sensors $\mathbf{s}$, as follows:

$$\mathbb{H}\big(p(\mathbf{x}_{k+1} \mid \mathbf{s}_k = \mathbf{s}, \ \mathbf{z}_{k+1}, \mathbf{s}_{0:k-1}, \mathbf{z}_{1:k})\big) = -\int_{\mathbb{X}} \log\big(p(\mathbf{x}_{k+1} \mid \mathbf{s}_k = \mathbf{s}, \mathbf{z}_{k+1}, \mathbf{s}_{0:k-1}, \mathbf{z}_{1:k})\big) \times p(\mathbf{x}_{k+1} \mid \mathbf{s}_k = \mathbf{s}, \mathbf{z}_{k+1}, \mathbf{s}_{0:k-1}, \mathbf{z}_{1:k})\, \mathrm{d}\mathbf{x}_{k+1} \tag{13}$$

Using the Bayes' rule and after some manipulations, the entropy can be derived as follows:

$$\begin{aligned}
&\mathbb{H}\big(p(\mathbf{x}_{k+1} \mid \mathbf{s}_k = \mathbf{s}, \mathbf{z}_{k+1}, \mathbf{s}_{0:k-1}, \mathbf{z}_{1:k})\big) \\
&= -\Bigg[\int_{\mathbb{X}} \Big(\log\big(p(\mathbf{z}_{k+1} \mid \mathbf{x}_{k+1}, \mathbf{s}_k = \mathbf{s})\, p(\mathbf{x}_{k+1} \mid \mathbf{s}_{0:k-1}, \mathbf{z}_{1:k})\big) \\
&\quad - \log\big(p(\mathbf{z}_{k+1} \mid \mathbf{s}_k = \mathbf{s}, \mathbf{s}_{0:k-1}, \mathbf{z}_{1:k})\big)\Big) \\
&\quad \times p(\mathbf{x}_{k+1} \mid \mathbf{s}_k = \mathbf{s}, \mathbf{z}_{k+1}\mathbf{s}_{0:k-1}, \mathbf{z}_{1:k})\, \mathrm{d}\mathbf{x}_{k+1}\Bigg] \\
&= -\int_{\mathbb{X}} \log\big(p(\mathbf{z}_{k+1} \mid \mathbf{x}_{k+1}, \mathbf{s}_k = \mathbf{s}) p(\mathbf{x}_{k+1} \mid \mathbf{s}_{0:k-1}, \mathbf{z}_{1:k})\big) \\
&\quad \times p(\mathbf{x}_{k+1} \mid \mathbf{s}_k = \mathbf{s}, \mathbf{z}_{k+1}, \mathbf{s}_{0:k-1}, \mathbf{z}_{1:k})\, \mathrm{d}\mathbf{x}_{k+1} \\
&\quad + \log\big(p(\mathbf{z}_{k+1} \mid \mathbf{s}_k = \mathbf{s}, \mathbf{s}_{0:k-1}, \mathbf{z}_{1:k})\big) \\
&\quad \times \int_{\mathbb{X}} p(\mathbf{x}_{k+1} \mid \mathbf{s}_k = \mathbf{s}, \mathbf{z}_{k+1}, \mathbf{s}_{0:k-1}, \mathbf{z}_{1:k})\, \mathrm{d}\mathbf{x}_{k+1}
\end{aligned} \tag{14}$$

We aim to express the entropy in terms of particles and weights. Therefore, the entropy of the predicted posterior state distribution at time $k+1$ given the predicted observations generated from the subset of sensor $\mathbf{s}$ according to (14) can be computed as follows:

$$\begin{aligned}
&\mathbb{H}\big(p(\mathbf{x}_{k+1} \mid \mathbf{s}_k = \mathbf{s}, \mathbf{z}_{k+1}, \mathbf{s}_{0:k-1}, \mathbf{z}_{1:k})\big) \\
&= -\sum_{i=1}^{N} \log\big(p(\mathbf{z}^i_{k+1} \mid \mathbf{x}^i_{k+1}, \mathbf{s}_k = \mathbf{s})\, \omega^i_k\big)\, \omega^i_{k+1} \\
&\quad + \underbrace{\log\big(p(\mathbf{z}_{k+1} \mid \mathbf{s}_k = \mathbf{s}, \mathbf{s}_{0:k-1}, \mathbf{z}_{1:k})\big)}_{\text{constant}} \underbrace{\sum_{i=1}^{N} \omega^i_{k+1}}_{=1}\Bigg] \\
&\approx -\sum_{i=1}^{N} \log\big(p(\mathbf{z}^i_{k+1} \mid \mathbf{x}^i_{k+1}, \mathbf{s}_k = \mathbf{s})\, \omega^i_k\big)\, \omega^i_{k+1}
\end{aligned} \tag{15}$$

where $p(\mathbf{z}^i_{k+1} \mid \mathbf{x}^i_{k+1}, \mathbf{s}_k = \mathbf{s})$ can be computed according to the measurement model in Eq. (5). By using this particle-based entropy, we will be able to predict the uncertainty associated with real-time state estimation using the measurements to be collected from any subset of sensors $\mathbf{s}$ at all time-steps. A high entropy value indicates high uncertainty in state estimation, whereas a low entropy value indicates a precise state estimation given the observations from the subset of sensors $\mathbf{s}$. Therefore, according to Eq. (6), the optimal subset of sensors $\mathbf{s}^*_k$ that minimizes the entropy in the estimation of the state will be selected for monitoring the coupled multidisciplinary system at the next time-step. After selecting $\mathbf{s}^*_k$, the corresponding measurements $\mathbf{z}_{k+1}$ will be obtained. Then, the unnormalized weights get updated as follows:

$$\tilde{\omega}^i_{k+1} \propto p(\mathbf{z}_{k+1} \mid \mathbf{x}^i_{k+1}, \mathbf{s}_k = \mathbf{s}^*_k)\, \omega^i_k \tag{16}$$

and accordingly, the normalized weights are obtained as follows:

$$\omega^i_{k+1} = \frac{\tilde{\omega}^i_{k+1}}{\sum_{j=1}^{N} \tilde{\omega}^j_{k+1}} \tag{17}$$

Finally, we achieve the state particles and their associated weights at time $k+1$, i.e., $\{\mathbf{x}^i_{k+1}, \omega^i_{k+1}\}_{i=1}^{N}$, and this process continues until the budget for monitoring the coupled multidisciplinary system terminates. It should be noted that the particles at $k=0$ are drawn from the initial state distribution π_0 and the initial particle weights are set to $\frac{1}{N}$. The algorithm of the proposed framework is presented in Algorithm 1.

Algorithm 1 Proposed Particle-Based Sensor Selection Framework

1: $\mathbf{x}^i_0 \sim \pi_0$, $\omega^i_0 = \frac{1}{N}$, for $i = 1, \ldots, N$
2: **for** $k = 1, 2, \ldots$ **do**
3: $\quad \mathbf{x}^i_k = f(\mathbf{x}^i_{k-1}, \mathbf{v}^i_k)$, for $i = 1, \ldots, N$ ▷ $\mathbf{v}^i_k \sim p_{\mathbf{v}}$
4: $\quad$ **for** $\forall \mathbf{s} \in \mathbb{S}$ **do**
5: $\quad\quad \mathbf{z}^i_k = h(\mathbf{x}^i_k, \mathbf{s}_{k-1} = \mathbf{s}, \mathbf{w}^i_k)$ ▷ $\mathbf{w}^i_k \sim p_{\mathbf{w}}$
6: $\quad\quad \tilde{\omega}^i_k = p(\mathbf{z}^i_k \mid \mathbf{x}^i_k, \mathbf{s}_{k-1} = \mathbf{s})\, \omega^i_{k-1}$, for $i = 1, \ldots, N$
7: $\quad\quad \omega^i_k = \tilde{\omega}^i_k / \sum_{j=1}^{N} \tilde{\omega}^j_k$, for $i = 1, \ldots, N$
8: $\quad\quad \mathbb{H}\big(p(\mathbf{x}_k \mid \mathbf{s}_{k-1} = \mathbf{s}, \mathbf{z}_k, \mathbf{s}_{0:k-2}, \mathbf{z}_{1:k-1})\big)$
$\quad\quad\quad = -\sum_{i=1}^{N} \log\big(p(\mathbf{z}^i_k \mid \mathbf{x}^i_k, \mathbf{s}_{k-1} = \mathbf{s})\, \omega^i_{k-1}\big)\, \omega^i_k$
9: $\quad$ **end for**
10: $\quad \mathbf{s}^*_{k-1} = \underset{\mathbf{s} \in S}{\operatorname{argmin}}\, \mathbb{H}\big(p(\mathbf{x}_k \mid \mathbf{s}_{k-1} = \mathbf{s}, \mathbf{z}_k, \mathbf{s}_{0:k-2}, \mathbf{z}_{1:k-1})\big)$
11: $\quad$ Collect observation $\mathbf{z}_k$ associated with the selected sensors $\mathbf{s}^*_{k-1}$
12: $\quad \tilde{\omega}^i_k = p(\mathbf{z}_k \mid \mathbf{x}^i_k, \mathbf{s}_{k-1} = \mathbf{s}^*_{k-1})\, \omega^i_{k-1}$, for $i = 1, \ldots, N$.
13: $\quad \omega^i_k = \tilde{\omega}^i_k / \sum_{j=1}^{N} \tilde{\omega}^j_k$, for $i = 1, \ldots, N$.
14: **end for**

3 Numerical Experiments

In this section, we demonstrate the performance of the proposed particle-based sensor selection framework for dynamically selecting the most informative sensors to monitor coupled multidisciplinary

Downloaded from http://asmedigitalcollection.asme.org/computingengineering/article-pdf/24/9/091001/7347527/jcise_24_9_091001.pdf by guest on 07 September 2024

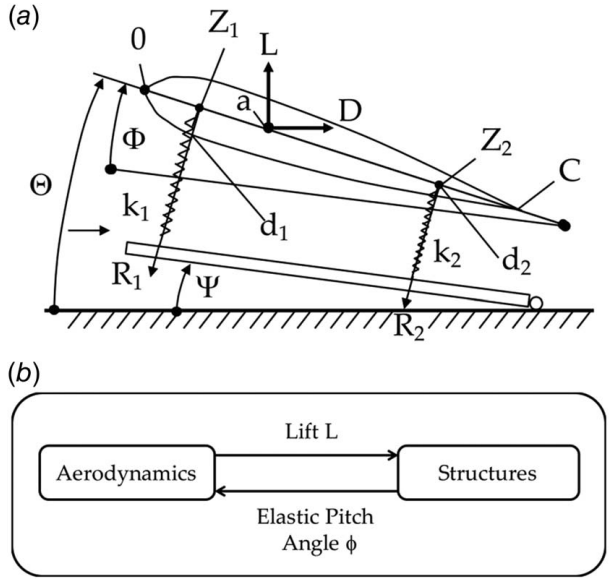

Fig. 2 (*a*) Coupled aerodynamics–structures system and (*b*) block diagram of the coupled aerodynamics-structures system, adapted from Ref. [46]

systems. The proposed framework is implemented on a coupled aerodynamics–structures system and a heart dipole problem.

3.1 Coupled Aerodynamics–Structures System. In this part of numerical experiments, a two-dimensional airfoil in airflow adapted from Ref. [46] is considered as a coupled two-disciplinary system. Figure 2(*a*) demonstrates this system in which the airfoil is supported by two linear springs attached to a ramp and the airfoil is permitted to pitch and plunge, and Fig. 2(*b*) shows the block diagram of this system. A complete description of the problem can be found in Ref. [46]. As it can be seen in Fig. 2(*b*), the coupling variables are the lift, L, and the elastic pitch angle, ϕ, which are the system states represented as follows:

$$L_k = qBC\left(2\pi(\phi_{k-1}+\psi) + r\left[1-\cos\left(\frac{\pi}{2}\frac{(\phi_{k-1}+\psi)}{\theta_0}\right)\right]\right) + v_{L,k},$$
$$\phi_k = \left(\frac{L_{k-1}}{k_1(1+p)} - \frac{L_{k-1}\,p}{k_2(1+p)}\right)\frac{1}{C(\bar{z}_2-\bar{z}_1)} + v_{\phi,k} \tag{18}$$

where $B = 100$, $q = 1\,\mathrm{N/cm^2}$, $C(\mathrm{chord}) = 10\,\mathrm{cm}$, $\psi = 0.05\,\mathrm{rad}$, $r = 0.9425$, $\theta_0 = 0.26\,\mathrm{rad}$, $p = 0.1111$, $k_1 = 4000\,\mathrm{N/cm}$, $k_2 = 2000\,\mathrm{N/cm}$, $\bar{z}_1 = 0.2$, and $\bar{z}_2 = 0.7$. The state noises are considered to be unbiased and normally distributed as $v_{L,k} \sim \mathcal{N}(0, \sigma^2_{v_L})$ and $v_{\phi,k} \sim \mathcal{N}(0, \sigma^2_{v_\phi})$, where $\sigma^2_{v_L} = 10$ and $\sigma^2_{v_\phi} = 10^{-6}$. In this experiment, the number of particles, N, is set to 10^6 and the initial state distribution, π_0, is considered to be $\mathcal{N}\left(\begin{bmatrix}70\\1\end{bmatrix}, \begin{bmatrix}1 & 0\\0 & 10^{-2}\end{bmatrix}\right)$. There are three sensors that provide noisy measurements of L, ϕ, and $L+\phi$ as follows:

$$\mathbf{z}_k = \begin{bmatrix} L_k + w_{L,k} \\ \phi_k + w_{\phi,k} \\ L_k + \phi_k + w_{L+\phi,k} \end{bmatrix} \tag{19}$$

where $w_{L,k} \sim \mathcal{N}(0, \sigma^2_{w_L})$, $w_{\phi,k} \sim \mathcal{N}(0, \sigma^2_{w_\phi})$, and $w_{L+\phi,k} \sim \mathcal{N}(0, \sigma^2_{w_{L+\phi}})$ with measurement noise variances $\sigma^2_{w_L}$, $\sigma^2_{w_\phi}$, and $\sigma^2_{w_{L+\phi}}$, respectively. In the following parts, experiments are implemented to illustrate the efficacy of the presented framework and the impact of measurement noises on the performance of the proposed method. The proposed framework is compared with two other scenarios. In the first scenario, called "All," observations from all available sensors in the system are collected at each time-step. In the second scenario, called "Random," only one sensor is selected randomly to monitor part of the system at each time-step. In our method, we consider two scenarios: one is observing only one sensor at each time-step, and the other is to observe two sensors out of three available sensors according to the proposed framework.

In the first part of the numerical experiments, we investigate the effectiveness of the proposed framework in the estimation of the state distribution after monitoring the selected optimal subsets with "one" and "two" sensors. The measurement noise variances are considered to be $\sigma^2_{w_L} = 1$, $\sigma^2_{w_\phi} = 2\times10^{-7}$, and $\sigma^2_{w_{L+\phi}} = 1$. Figure 3 shows the particles and the 95% confidence intervals associated with the true state distributions and the estimated distributions at time-steps (*a*) 2, (*b*) 10, and (*c*) 20, after monitoring the sensors selected by the proposed framework and "All" and "Random" sensor selection policies. At all time-steps, it can be seen that observing "All" available sensors results in the most accurate estimation of the true state distribution. Nevertheless, this is achieved at the expense of increased processing time and resource utilization due to the computational/economic demands involved in observing all available sensors. On the other hand, the "Random" policy results in the least accurate estimation as it does not take into account the informativeness of the sensor in the selection process and acquiring the observation. However, it can be seen that the proposed framework in both cases of selecting one and two sensors outperforms the random selection strategy and performs

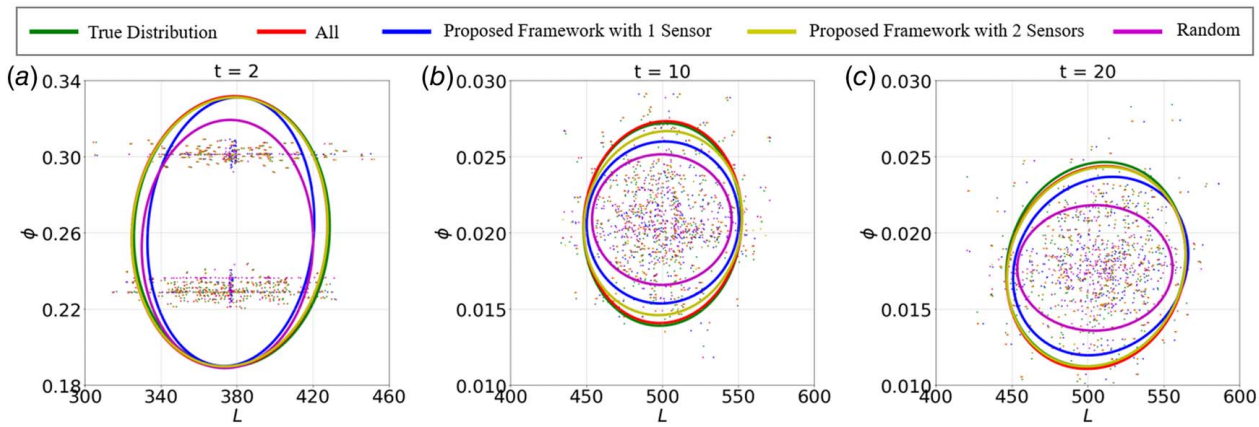

Fig. 3 The particles and the 95% confidence intervals associated with the true state distributions and the estimated distributions at time-steps: (*a*) 2, (*b*) 10, and (c) 20, after monitoring "one" and "two" sensors selected by the proposed framework and "All" and "Random" sensor selection policies in the coupled aerodynamics-structures system

Downloaded from http://asmedigitalcollection.asme.org/computingengineering/article-pdf/24/9/091001/7347527/jcise_24_9_091001.pdf by guest on 07 September 2024

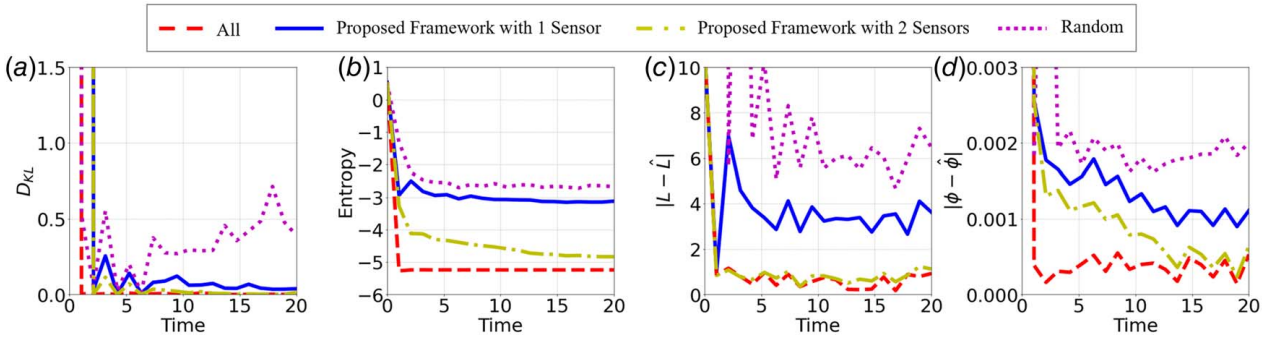

Fig. 4 (*a*) The Kullback–Leibler divergence (D_{KL}) between the true and the estimated state distributions, (*b*) average entropy of the state particles, (*c*), and (*d*) average absolute errors between the true and the estimated states L and ϕ, at each time-step obtained by the "proposed framework" when choosing one or two sensors, and two scenarios of "All" and "Random" sensor selection, over 300 independent runs for the coupled aerodynamics–structures system

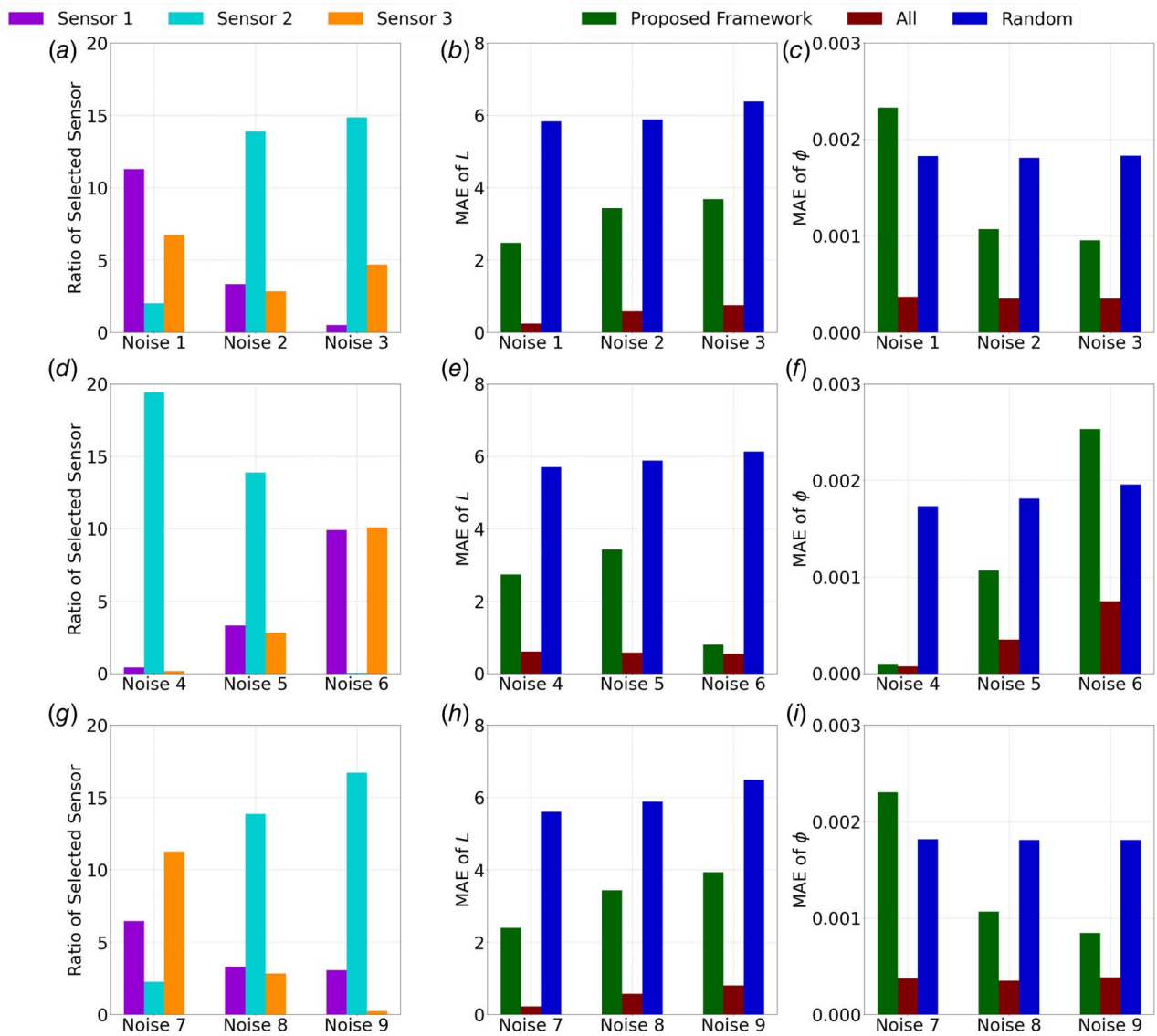

Fig. 5 First column (*a*, *d*, *g*): ratio of each sensor (1, 2, and 3) with different measurement noise selected by the proposed framework in 20 time-steps, averaged over 100 independent runs; second (*b*, *e*, *h*) and third columns (*c*, *f*, *i*): mean average error (MAE) of L and ϕ for different values of measurement noises (noise 1–9) over 100 independent runs of the "proposed framework" and two scenarios of "All" and "Random" sensor selection in the coupled aerodynamics–structures system

Downloaded from http://asmedigitalcollection.asme.org/computingengineering/article-pdf/24/9/091001/7347527/jcise_24_9_091001.pdf by guest on 07 September 2024

close to the case of monitoring all available sensors while offering substantial potential in reducing computational costs.

Figure 4 demonstrates the state estimation accuracy achieved by the proposed framework selecting one and two sensors and the "All" and "Random" sensor selection policies, in terms of (*a*) Kullback–Leibler divergence (D_{KL}), (*b*) average entropy, and (*c*) and (*d*) average absolute errors of estimated states. D_{KL} is a quantity used to measure the distance between two probability distributions P and Q, defined as follows:

$$D_{\mathrm{KL}}(P \parallel Q) = \int_{-\infty}^{\infty} p(x) \log\left(\frac{p(x)}{q(x)}\right) \mathrm{d}x \tag{20}$$

where p and q denote the probability densities of P and Q. In all the numerical experiments, we approximate the true and the estimated state distributions with multivariate normal distributions, where the KL divergence can be computed as follows:

$$D_{\mathrm{KL}}(P \parallel Q) = \frac{1}{2}\left[(\boldsymbol{\mu}_2 - \boldsymbol{\mu}_1)^T \Sigma_2^{-1}(\boldsymbol{\mu}_2 - \boldsymbol{\mu}_1) + Tr(\Sigma_2^{-1}\Sigma_1) + \ln\frac{\det\Sigma_2}{\det\Sigma_1} - n\right] \tag{21}$$

where $P \sim \mathcal{N}(\boldsymbol{\mu}_1, \Sigma_1)$ and $Q \sim \mathcal{N}(\boldsymbol{\mu}_2, \Sigma_2)$ and n is the dimension of these multivariate normal distributions.

Figure 4(*a*) represents D_{KL} as a measure of distance between the true and the estimated state distributions derived from observing different sets of sensors selected by each method over time. The smaller values of D_{KL} indicate the closeness of the true and the estimated state distributions, therefore reflecting the accuracy of the estimation process. As expected, monitoring all available sensors and monitoring one sensor randomly have respectively achieved the smallest and the largest D_{KL} values. It can be seen that the D_{KL} values obtained by the proposed framework in both cases of selecting one and two sensors are considerably small, which demonstrates the effectiveness of the proposed framework in monitoring coupled multidisciplinary systems with lower computational cost.

Figure 4(*b*) presents the entropy of the state particles at each time-step, averaged over 300 independent runs obtained by the proposed framework after monitoring one and two sensors and the two scenarios of "All" and "Random" sensor selection. The entropy serves as a measure of the amount of uncertainty associated with the estimated state and quantifies the amount of information needed to describe the probability distribution of the state. High entropy indicates greater uncertainty, while low entropy implies more certainty in the estimation process. It can be seen that observing all three sensors has achieved the minimum entropy values at all time-steps, and randomly selecting one sensor has resulted in the maximum entropy value. However, the proposed framework, by selecting only one informative sensor among all available sensors, achieves a lower entropy in state estimation compared to the random scenario. Consistent with expectations, observing two sensors by the proposed framework yields smaller entropy values and more desirable results, lying between observing "All" and one sensor by our method, with a closer trajectory to the "All" sensor selection scenario. This demonstrates the superiority of the proposed framework compared to other scenarios, in which the entropy of the state particles is reduced by observing only the most informative sensor. As explained earlier, higher entropy represents a higher uncertainty in the state estimation. It is shown that the proposed framework achieves a remarkable level of accuracy with high robustness and low computational cost. It should be noted that the proposed framework can be generalized to the selection of any number of sensors among the available ones.

Figures 4(*c*) and 4(*d*) illustrate the average absolute errors between the true and the estimated state of the system over 300 independent runs. In accordance with the previous results, observing "All" sensors yields the smallest error values in the estimation of both L and ϕ, while "Random" observation has the highest error values among all methods. The estimation errors after observing the sensors selected by the proposed method are within these two extremes, showing a satisfactory level of accuracy and tending to the lower error boundaries in estimating the state of the system.

In the next part of numerical experiments, we evaluate the impact of various measurement noises on the sensor selection and the state estimation accuracy. For this evaluation, we consider a set of nine various measurement noises corresponding to the three available sensors. Let $\boldsymbol{\sigma}^2$ contain the measurement noise variances, defined in (19), as follows:

$$\boldsymbol{\sigma}^2 = \begin{bmatrix} \sigma^2_{w_L} \\ \sigma^2_{w_\phi} \\ \sigma^2_{w_{L+\phi}} \end{bmatrix}$$

We consider the following measurement noise variances for the sensors:

$$\text{Noise 1} = \begin{bmatrix} 0.1 \\ 2\times10^{-7} \\ 1 \end{bmatrix} \quad \text{Noise 2} = \begin{bmatrix} 1 \\ 2\times10^{-7} \\ 1 \end{bmatrix} \quad \text{Noise 3} = \begin{bmatrix} 10 \\ 2\times10^{-7} \\ 1 \end{bmatrix}$$

$$\text{Noise 4} = \begin{bmatrix} 1 \\ 10^{-8} \\ 1 \end{bmatrix} \quad \text{Noise 5} = \begin{bmatrix} 1 \\ 2\times10^{-7} \\ 1 \end{bmatrix} \quad \text{Noise 6} = \begin{bmatrix} 1 \\ 10^{-6} \\ 1 \end{bmatrix}$$

$$\text{Noise 7} = \begin{bmatrix} 1 \\ 2\times10^{-7} \\ 0.1 \end{bmatrix} \quad \text{Noise 8} = \begin{bmatrix} 1 \\ 2\times10^{-7} \\ 1 \end{bmatrix} \quad \text{Noise 9} = \begin{bmatrix} 1 \\ 2\times10^{-7} \\ 10 \end{bmatrix}$$

where in each row, the noise variance of the corresponding sensor varies while maintaining a constant value for the other two to examine the effect of each sensor's measurement noise on sensor selection and state estimation.

Figure 5 presents the results obtained by the proposed framework selecting one sensor and the "All" and "Random" sensor selection strategies for different values of measurement noises (noise 1–9) over 100 independent runs of the coupled aerodynamics-structures system in 20 time-steps. Figures 5(*a*), 5(*d*), and 5(*g*) show the ratio of each sensor with different measurement noise selected by the proposed framework in 20 time-steps, averaged over 100 independent runs. As noted earlier, in rows 1, 2, and 3, the noise associated with sensors 1, 2, and 3 increases, respectively, while others remain constant. As can be seen, the increase in the noise variance of each sensor results in a decrease in the selection rate associated with that sensor. For instance, in Fig. 5(*a*), as sensor 1 has the smallest variance ($\sigma^2_{w_L}$) in Noise 1, it has the highest selection ratio compared to noise 2 and 3 as it provides more informative observation, and as its

Downloaded from http://asmedigitalcollection.asme.org/computingengineering/article-pdf/24/9/091001/7347527/jcise_24_9_091001.pdf by guest on 07 September 2024

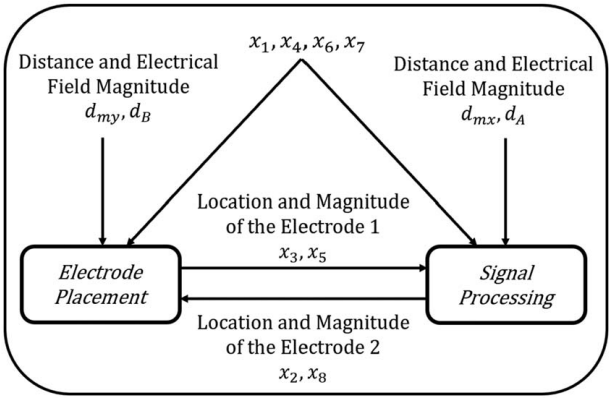

Fig. 6 Block diagram of the heart dipole problem, adapted from Ref. [47]

uncertainty in the corresponding measurement increases, the selection ratio for this sensor decreases and for other sensors increases.

Furthermore, as a sensor is more frequently chosen, there is a corresponding decrease in the error of estimating the state associated with the sensor. This is reflected in the second and third columns of Fig. 5, where the mean average errors (MAEs) between the true and the estimated state values of L and ϕ obtained by the proposed framework and two scenarios of "All" and "Random" are compared for different measurement noises. It can be seen that the proposed framework achieves reasonably high accuracy, i.e., low MAE, in estimating the system states by selecting only one, that is the most informative, sensor with estimation errors that are comparable to the "All" scenario. It should be emphasized that in the "All" scenario, all three sensors are observed for the state estimation, while in the proposed framework, only one sensor is selected for acquiring a measurement. Consistent with the previous results and as expected, the "Random" scenario has the highest estimation error unless a sensor is not frequently selected in the proposed framework because of the corresponding high measurement noise. This can be seen, for instance, in noise 6 in Fig. 5(*f*), where the MAE of ϕ obtained by the proposed framework is higher than the random selection scenario as shown in noise 6 in Fig. 5(*d*), the selection ratio of sensor 2 is noticeably small.

It is important to emphasize that the proposed framework prioritizes minimizing system-level uncertainty, quantified in terms of entropy, through the intelligent selection of sensors. The observed higher mean average error in some cases is attributed to the inherent characteristics of the sensors, particularly the noise levels of sensors and their informativeness. In scenarios where certain sensors are not selected for measurement due to their low informativeness or high noise levels, the corresponding state variables exhibit higher errors compared to those where sensors have been selected. However, it is crucial to emphasize that the proposed method aims to minimize the overall entropy of the posterior distribution of the state variables, thereby enhancing the overall estimation performance of the system. It is also worth noting that the proposed method can be adapted to minimize the entropy of the marginalized state distributions, accounting for the importance of states to be estimated accurately instead of the entropy of the joint distribution. By incorporating this refinement, the framework can prioritize reducing uncertainty in critical state variables while ensuring that less critical variables are adequately estimated, allowing for a more targeted sensor selection strategy tailored to the specific requirements and objectives of the system under consideration.

3.2 Heart Dipole Problem. The heart dipole problem represents a well-established test case in the field of multidisciplinary design optimization, originally introduced in the literature by NASA [47]. This problem involves the experiment of measuring a synthetic dipole moment generated by a human heart through the use of two artificial dipoles contained within an electrolyte disk. The human heart dipole has been converted into a test problem for multidisciplinary system analysis methods by defining two disciplines, shown in Fig. 6. In this problem, the two disciplines are structured to address different aspects of the measurement process. The first discipline focuses on optimizing the placement of artificial electrodes within an electrolyte disk to simulate the measurement of the dipole moment generated by a human heart. This discipline, known as electrode placement, focuses on determining the optimal locations and orientations of the electrodes to maximize the accuracy and reliability of the measured signal while minimizing interference and noise. The second discipline involves signal processing techniques applied to the recorded data from the electrodes. This discipline, called signal processing, encompasses various methods, such as filtering, feature extraction, and signal reconstruction, aimed at extracting meaningful information about the dipole moment parameters from the recorded signals. Optimizing electrode placement and signal processing disciplines enables a comprehensive analysis and enhancement of the measurement system's performance in capturing the underlying physiological activity of the heart. This problem can be stated as a set of four nonlinear equations and eight variables ($x_1, \ldots, x_8$ as coordinates and magnitudes of each dipole on x and y axis), where four variables (x_1, x_4, x_6 and x_7) and four pieces of measured data (parameters d_{mx}, d_{my}, d_A and d_B) are the inputs to the system, and four variables (x_2, x_3, x_5, and x_8) are the coupling variables [48], which define the system state, represented as follows:

$$\begin{aligned} x_{2,k} &= -x_1 + d_{mx} + v_{1,k}, \\ x_{3,k} &= -x_4 + d_{my} + v_{2,k}, \\ x_{5,k} &= \frac{-x_7\, x_1 - x_{8,k-1}\, x_{2,k-1} - x_6\, x_4 + d_B}{x_{3,k-1}} + v_{3,k}, \\ x_{8,k} &= \frac{x_{5,k-1}\, x_1 + x_6\, x_{2,k-1} - x_7\, x_{3,k-1} - d_A}{x_4} + v_{4,k} \end{aligned} \tag{22}$$

where d_{mx} and d_{my} are the minimum distance between the dipole source and the inner/outer surface, respectively, and d_A and d_B are the measured values of the electrical field at the surface, respectively. In this experiment, $d_{mx} = d_{my} = d_A = d_B = 1$, $x_1 = 6.43 \times 10^{-4}$, $x_4 = -0.46$, $x_6 = 1$, and $x_7 = 3.47 \times 10^{-4}$ are constant inputs to the system, and the state noises are considered as unbiased and normally distributed as $v_{1,k} \sim \mathcal{N}(0, \sigma_{v_1}^2)$, $v_{2,k} \sim \mathcal{N}(0, \sigma_{v_2}^2)$, $v_{3,k} \sim \mathcal{N}(0, \sigma_{v_3}^2)$, and $v_{4,k} \sim \mathcal{N}(0, \sigma_{v_4}^2)$. The states are partially observable through noisy sensor measurements as follows:

$$\mathbf{z}_k = \begin{bmatrix} x_{5,k} + w_{1,k} \\ x_{8,k} + w_{2,k} \\ x_{5,k} + x_{8,k} + w_{3,k} \\ x_{5,k}^2 + w_{4,k} \end{bmatrix}$$

where $w_{1,k} \sim \mathcal{N}(0, \sigma_{w_1}^2)$, $w_{2,k} \sim \mathcal{N}(0, \sigma_{w_2}^2)$, $w_{3,k} \sim \mathcal{N}(0, \sigma_{w_3}^2)$, $w_{4,k} \sim \mathcal{N}(0, \sigma_{w_4}^2)$. In this experiment, we consider the number of particles (N) to be 1, 000, 000, and the state noise, measurement noise, and the initial state distribution are as follows:

State noise variances: $\sigma_{v_1}^2 = 10^{-2}$, $\sigma_{v_2}^2 = 10^{-2}$, $\sigma_{v_3}^2 = 10^{-2}$, $\sigma_{v_4}^2 = 10^{-4}$

Measurement noise variances: $\sigma_{w_1}^2 = 10^{-2}$, $\sigma_{w_2}^2 = 10^{-4}$, $\sigma_{w_3}^2 = 1$, $\sigma_{w_4}^2 = 1$

Initial state distribution (π_0): $\mathcal{N}\left(\begin{bmatrix} 10 \\ 15 \\ 0.1 \\ 50 \end{bmatrix}, \begin{bmatrix} 1 & 0 & 0 & 0 \\ 0 & 1 & 0 & 0 \\ 0 & 0 & 1 & 0 \\ 0 & 0 & 0 & 1 \end{bmatrix} \right)$

We implement the proposed sensor selection approach on the heart dipole problem to demonstrate its performance in the state

Downloaded from http://asmedigitalcollection.asme.org/computingengineering/article-pdf/24/9/091001/7347527/jcise_24_9_091001.pdf by guest on 07 September 2024

estimation of this coupled multidisciplinary system given noisy measurement from a single selected sensor at each time. Similar to previous experiments, the proposed framework is compared to two scenarios of "All" and "Random" sensor selection. In the "All" scenario, all four sensors are observed simultaneously at each time-step, and their measurements are used for state estimation. In the "Random" scenario, one sensor is selected randomly to acquire an observation, regardless of the amount of information the sensor provides.

Figure 7 presents the results obtained over 500 independent runs of the heart dipole problem in 20 time-steps. Figure 7(*a*) shows the ratio of each sensor selected by the proposed framework in 20 time-steps, averaged over 500 independent runs. It can be seen that sensors 1 and 2 have been chosen more frequently, indicating that they possess the highest information compared to the other two sensors. This serves as the advantage of the proposed approach, as it eliminates the necessity of allocating computational resources toward noninformative sensors. It should be noted that the computational cost associated with acquiring measurements from all sensors is four times of the proposed framework and the random selection strategy, as in the latter cases, only one measurement from a single sensor is acquired.

Figure 7(*b*) illustrates the entropy of the state particles at each time-step averaged over 500 independent runs of sensor selection by the proposed framework as well as the two scenarios of "All" and "Random" sensor selection. It is seen that the entropy values at each time-step obtained by the proposed method fall between the entropy values obtained by the "All" and "Random" sensor selection methods. It is essential to acknowledge that while the proposed method has not achieved the same level of entropy reduction as scenario "All" and it is closer to the "Random" entropy levels, it has achieved a high efficiency in estimating the state distribution by recognizing the most informative sensor at each time. This efficiency is demonstrated in Fig. 7(*c*) through the Kullback–Leibler divergence (D_{KL}) between the true and the estimated state distributions at each time-step over 500 independent runs. It can be seen that the scenario of observing all available sensors achieves the minimum D_{KL} values, while the "Random" sensor selection yields significantly higher D_{KL} values. Notably, in this result, one can observe that the proposed framework has achieved D_{KL} values close to "All" scenario. This result illustrates that the proposed method has been effective in state estimation with a high accuracy level by observing only one informative sensor instead of all four available sensors.

In this part of numerical experiments, we evaluate the performance of the proposed framework in the presence of different combinations of sensors monitoring the heart dipole problem. The experiment considers various configurations of available sensors to monitor the coupled multidisciplinary system. The proposed framework is implemented to select the most informative sensor among all available ones. Table 1 presents the average entropy of state particles per step and mean absolute error of state per step over 500 independent runs for various combinations of available sensors in the heart dipole problem. As with previous experiments, the proposed framework is compared to two other scenarios, "All" and "Random" sensor selection. The average entropy values are

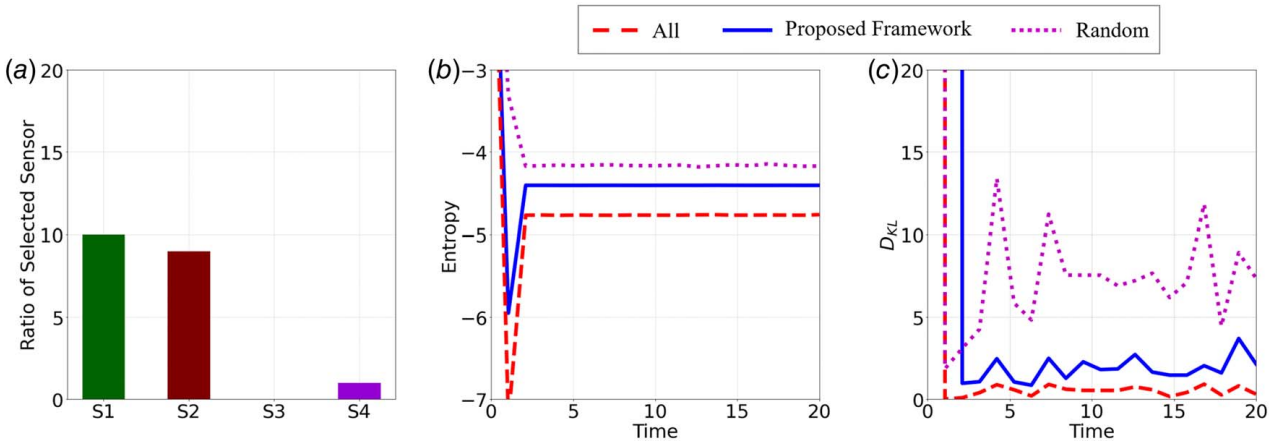

Fig. 7 (*a*) The ratio of each sensor (1, 2, 3, and 4) selected by the proposed framework, (*b*) average entropy of the state particles over time, and (c) the Kullback–Leibler divergence (D_{KL}) between the true and the estimated state distributions, over 500 independent runs of the "Proposed Framework" and two scenarios of "All" and "Random" sensor selection for the heart dipole problem in 20 time-steps

Table 1 The average entropy per step of the state particles and mean absolute error of state per step over 500 independent runs, for different combinations of available sensors obtained by the "Proposed Framework" and two scenarios of "All" and "Random" sensor selection in the heart dipole problem

	Average entropy per step			Mean absolute error of state per step		
Available sensors	Proposed framework	All	Random	Proposed framework	All	Random
*S*1, *S*2, *S*3, *S*4	−4.4911	−4.8507	−4.2226	0.0717	0.0617	0.0925
*S*1, *S*2, *S*3	−4.3976	−4.7481	−4.2342	0.0751	0.0647	0.0991
*S*1, *S*2, *S*4	−4.4805	−4.8482	−4.2972	0.0730	0.0617	0.0872
*S*1, *S*3, *S*4	−4.4910	−4.5032	−4.1861	0.0648	0.0641	0.0903
*S*2, *S*3, *S*4	−4.4910	−4.5318	−4.1682	0.0822	0.0801	0.1037
*S*1, *S*2	−4.3978	−4.7454	−4.3624	0.0749	0.0649	0.0847
*S*1, *S*3	−4.3979	−4.4006	−4.1854	0.0673	0.0672	0.0919
*S*1, *S*4	−4.4704	−4.5015	−4.2901	0.064	0.0634	0.0752
*S*2, *S*3	−4.3184	−4.3329	−4.1488	0.1042	0.1101	0.1083
*S*2, *S*4	−4.4911	−4.5271	−4.2562	0.1030	0.0810	0.0941
*S*3, *S*4	−4.1792	−4.1838	−4.0858	0.0833	0.0833	0.0970

Downloaded from http://asmedigitalcollection.asme.org/computingengineering/article-pdf/24/9/091001/7347527/jcise_24_9_091001.pdf by guest on 07 September 2024

computed to assess the performance of the proposed framework in minimizing the uncertainty in the state estimation process, and the mean absolute errors quantify the accuracy of the state estimation. The results show that the proposed framework, which selects only one informative sensor, achieves both low uncertainty and high accuracy in state estimation. This performance is comparable to the scenario where all available sensors are selected and surpasses the performance of the random selection method. It can be seen that regardless of the sensor combination or the presence/absence of any specific sensor, the proposed framework consistently identifies the most informative sensor among the available ones. These results demonstrate the adaptability and generalizability of the proposed framework across different monitoring scenarios and highlight its capability to maintain estimation accuracy while optimizing resource efficiency.

4 Conclusion

This article presented a dynamic sensor selection approach for efficient monitoring of partially observable coupled multidisciplinary systems. In many multidisciplinary systems, a vast array of sensors is employed to capture various aspects of the system's behavior. However, analyzing data from all sensors can be computationally intensive and time consuming. To address this challenge, we proposed a sensor selection framework that identifies the most informative sensors for state estimation in real time, making a balance between estimation accuracy and resource efficiency. This is achieved through a particle-based Bayesian filtering technique that probabilistically predicts the uncertainty in the state estimation after monitoring any set of sensors. The efficiency, accuracy, and robustness of state estimation by the proposed framework are demonstrated in the numerical experiments. Future work will include enhancing the scalability of the proposed framework to accommodate larger-scale coupled multidisciplinary systems by integrating adaptive sampling strategies alongside approximate inference methods and optimized particle resampling techniques.

Funding Data

- This work was supported by the 10.13039/100006754 ARMY Research Laboratory (Award numbers W911NF2410098 and W911NF2320179).

Conflict of Interest

There are no conflicts of interest.

Data Availability Statement

The datasets generated and supporting the findings of this article are obtainable from the corresponding author upon reasonable request.

References

[1] Gray, J. S., Hwang, J. T., Martins, J. R., Moore, K. T., and Naylor, B. A., 2019, "OpenMDAO: An Open-Source Framework for Multidisciplinary Design, Analysis, and Optimization," Struct. Multidiscip. Optim., **59**, pp. 1075–1104.

[2] Mader, C. A., Kenway, G. K., Yildirim, A., and Martins, J. R., 2020, "ADflow: An Open-Source Computational Fluid Dynamics Solver for Aerodynamic and Multidisciplinary Optimization," J. Aerospace Inf. Syst., **17**(9), pp. 508–527.

[3] Ghoreishi, S. F., and Imani, M., 2021, "Bayesian Surrogate Learning for Uncertainty Analysis of Coupled Multidisciplinary Systems," ASME J. Comput. Inf. Sci. Eng., **21**(4), p. 041009.

[4] Hu, Z., and Mahadevan, S., 2017, "A Surrogate Modeling Approach for Reliability Analysis of a Multidisciplinary System With Spatio-Temporal Output," Struct. Multidiscipl. Optim., **56**, pp. 553–569.

[5] Asadi, N., and Ghoreishi, S. F., 2022, "Bayesian State Estimation in Partially-Observed Dynamic Multidisciplinary Systems," Frontiers Aerospace Eng., **1**, p. 1036642.

[6] Guan, X., Yang, B., Chen, C., Dai, W., and Wang, Y., 2016, "A Comprehensive Overview of Cyber-Physical Systems: From Perspective of Feedback System," IEEE/CAA J. Automatica Sinica, **3**(1), pp. 1–14.

[7] Allen, J. K., Nellippallil, A. B., Ming, Z., Milisavljevic-Syed, J., and Mistree, F., 2023, "Designing Evolving Cyber-Physical-Social Systems: Computational Research Opportunities," ASME J. Comput. Inf. Sci. Eng., **23**(6), p. 060815.

[8] Ghoreishi, S. F., and Imani, M., 2020, "Bayesian Optimization for Efficient Design of Uncertain Coupled Multidisciplinary Systems," 2020 American Control Conference (ACC), IEEE, pp. 3412–3418.

[9] Soria Zurita, N. F., Colby, M. K., Tumer, I. Y., Hoyle, C., and Tumer, K., 2018, "Design of Complex Engineered Systems Using Multi-agent Coordination," ASME J. Comput. Inf. Sci. Eng., **18**(1), p. 011003.

[10] DeCarlo, E. C., Mahadevan, S., and Smarslok, B. P., 2018, "Efficient Global Sensitivity Analysis With Correlated Variables," Struct. Multidiscipl. Optim., **58**, pp. 2325–2340.

[11] Friedman, S., Ghoreishi, S. F., and Allaire, D. L., 2017, "Quantifying the Impact of Different Model Discrepancy Formulations in Coupled Multidisciplinary Systems," 19th AIAA Non-Deterministic Approaches Conference, p. 1950.

[12] Hearn, T. A., Hendricks, E., Chin, J., and Gray, J. S., 2016, "Optimization of Turbine Engine Cycle Analysis With Analytic Derivatives," 17th AIAA/ISSMO Multidisciplinary Analysis and Optimization Conference, p. 4297.

[13] Ghoreishi, S. F., 2016, "Uncertainty Analysis for Coupled Multidisciplinary Systems Using Sequential Importance Resampling," Master's thesis.

[14] Hendricks, E. S., and Gray, J. S., 2019, "pyCycle: A Tool for Efficient Optimization of Gas Turbine Engine Cycles," Aerospace, **6**(8), p. 87.

[15] Baptista, R., Marzouk, Y., Willcox, K., and Peherstorfer, B., 2018, "Optimal Approximations of Coupling in Multidisciplinary Models," AIAA. J., **56**(6), pp. 2412–2428.

[16] Ghoreishi, S., and Allaire, D., 2017, "Adaptive Uncertainty Propagation for Coupled Multidisciplinary Systems," AIAA. J., **55**(11), pp. 3940–3950.

[17] Chaudhuri, A., Lam, R., and Willcox, K., 2018, "Multifidelity Uncertainty Propagation Via Adaptive Surrogates in Coupled Multidisciplinary Systems," AIAA. J., **56**(1), pp. 235–249.

[18] Yan, J., Xiang, R., Kamensky, D., Tolley, M. T., and Hwang, J. T., 2022, "Topology Optimization With Automated Derivative Computation for Multidisciplinary Design Problems," Struct. Multidiscipl. Optim., **65**(5), p. 151.

[19] Ghoreishi, S. F., and Allaire, D. L., 2016, "Compositional Uncertainty Analysis Via Importance Weighted Gibbs Sampling for Coupled Multidisciplinary Systems," 18th AIAA Non-Deterministic Approaches Conference, p. 1443.

[20] Chung, H., Hwang, J. T., Gray, J. S., and Kim, H. A., 2019, "Topology Optimization in OpenMDAO," Struct. Multidiscipl. Optim., **59**, pp. 1385–1400.

[21] Nagata, T., Yamada, K., Nakai, K., Saito, Y., and Nonomura, T., 2023, "Randomized Group-Greedy Method for Large-Scale Sensor Selection Problems," IEEE Sensors J., **23**, pp. 9536–9548.

[22] Nakai, K., Sasaki, Y., Nagata, T., Yamada, K., Saito, Y., and Nonomura, T., 2022, "Nondominated-Solution-based Multi-objective Greedy Sensor Selection for Optimal Design of Experiments," IEEE Trans. Signal Process., **70**, pp. 5694–5707.

[23] Kazeminajafabadi, A., and Imani, M., 2024, "Optimal Joint Defense and Monitoring for Networks Security Under Uncertainty: A POMDP-Based Approach," IET Information Security, **2024**, p. 7966713.

[24] Hashemi, A., Ghasemi, M., Vikalo, H., and Topcu, U., 2020, "Randomized Greedy Sensor Selection: Leveraging Weak Submodularity," IEEE. Trans. Automat. Contr., **66**(1), pp. 199–212.

[25] Smarra, F., Tjen, J., and D'Innocenzo, A., 2022, "Learning Methods for Structural Damage Detection Via Entropy-Based Sensors Selection," J. Robust. Nonlinear. Control., **32**(10), pp. 6035–6067.

[26] Kazeminajafabadi, A., and Imani, M., 2023, "Optimal Monitoring and Attack Detection of Networks Modeled by Bayesian Attack Graphs," Cybersecurity, **6**(1), p. 22.

[27] Saucan, A. A., and Win, M. Z., 2020, "Information-Seeking Sensor Selection for Ocean-of-Things," IEEE Internet Things J., **7**(10), pp. 10072–10088.

[28] Zheng, X., Wang, Y., Wang, L., Cai, R., Li, M., and Qiu, Y., 2023, "Data-Driven Sensor Selection for Signal Estimation of Vertical Wheel Forces in Vehicles," ASME J. Comput. Inf. Sci. Eng., **23**(3), p. 031010.

[29] Swischuk, R., and Allaire, D., 2019, "A Machine Learning Approach to Aircraft Sensor Error Detection and Correction," ASME J. Comput. Inf. Sci. Eng., **19**(4), p. 041009.

[30] Ostachowicz, W., Soman, R., and Malinowski, P., 2019, "Optimization of Sensor Placement for Structural Health Monitoring: A Review," Struct. Health. Monit., **18**(3), pp. 963–988.

[31] Zare, A., and Jovanović, M. R., 2018, "Optimal Sensor Selection Via Proximal Optimization Algorithms," 2018 IEEE Conference on Decision and Control (CDC), IEEE, pp. 6514–6518.

[32] Owais, M., Moussa, G. S., and Hussain, K. F., 2019, "Sensor Location Model for O/D Estimation: Multi-criteria Meta-Heuristics Approach," Oper. Res. Perspect., **6**, p. 100100.

[33] Gupta, V., Chung, T. H., Hassibi, B., and Murray, R. M., 2006, "On a Stochastic Sensor Selection Algorithm With Applications in Sensor Scheduling and Sensor Coverage," Automatica, **42**(2), pp. 251–260.

[34] Muradore, R., Bezzo, F., and Barolo, M., 2006, "Optimal Sensor Location for Distributed-Sensor Systems Using Multivariate Regression," Comput. Chem. Eng., **30**(3), pp. 521–534.

[35] Wang, Y., and Ma, X., 2012, "Optimal Sensor Selection for Wind Turbine Condition Monitoring Using Multivariate Principal Component Analysis Approach," 18th International Conference on Automation and Computing (ICAC), pp. 1–7.

Downloaded from http://asmedigitalcollection.asme.org/computingengineering/article-pdf/24/9/091001/7347527/jcise_24_9_091001.pdf by guest on 07 September 2024

[36] Alali, M., Kazeminajafabadi, A., and Imani, M., 2024, "Deep Reinforcement Learning Sensor Scheduling for Effective Monitoring of Dynamical Systems," Syst. Sci. Control Eng., **12**, p. 2329260.
[37] Leong, A. S., Ramaswamy, A., Quevedo, D. E., Karl, H., and Shi, L., 2020, "Deep Reinforcement Learning for Wireless Sensor Scheduling in Cyber-Physical Systems," Automatica, **113**, p. 108759.
[38] Kazeminajafabadi, A., Ghoreishi, S. F., and Imani, M., 2024, "Optimal Detection for Bayesian Attack Graphs Under Uncertainty in Monitoring and Reimaging," 2023 American Control Conference (ACC), IEEE.
[39] Ravari, A., Ghoreishi, S. F., and Imani, M., 2024, "Optimal Inference of Hidden Markov Models Through Expert-Acquired Data," IEEE Trans. Artif. Intell., pp. 1–15.
[40] Chamon, L. F., Pappas, G. J., and Ribeiro, A., 2020, "Approximate Supermodularity of Kalman Filter Sensor Selection," IEEE. Trans. Automat. Contr., **66**(1), pp. 49–63.
[41] Zhang, H., Ayoub, R., and Sundaram, S., 2017, "Sensor Selection for Kalman Filtering of Linear Dynamical Systems: Complexity, Limitations and Greedy Algorithms," Automatica, **78**, pp. 202–210.
[42] Peng, X., Zhang, B., and Rong, L., 2019, "A Robust Unscented Kalman Filter and Its Application in Estimating Dynamic Positioning Ship Motion States," J. Marine Sci. Technol., **24**, pp. 1265–1279.
[43] Asadi, N., Hosseini, S. H., Imani, M., Aldrich, D. P., and Ghoreishi, S. F., 2024, "Privacy-Preserved Federated Reinforcement Learning for Autonomy in Signalized Intersections," ASCE International Conference on Transportation and Development (ICTD), American Society of Civil Engineers.
[44] Ye, L., Woodford, N., Roy, S., and Sundaram, S., 2020, "On the Complexity and Approximability of Optimal Sensor Selection and Attack for Kalman Filtering," IEEE. Trans. Automat. Contr., **66**(5), pp. 2146–2161.
[45] Asadi, N., and Ghoreishi, S. F., 2022, "Input Distribution Estimation in Dynamic Coupled Multidisciplinary Systems," 2022 56th Asilomar Conference on Signals, Systems, and Computers, IEEE, pp. 65–70.
[46] Sobieszczanski-Sobieski, J., 1990, "Sensitivity of Complex, Internally Coupled Systems," AIAA J., **28**(1), pp. 153–160.
[47] Padula, S., Alexandrov, N., and Green, L., 1996, "MDO Test Suite at NASA Langley Research Center," 6th Symposium on Multidisciplinary Analysis and Optimization, p. 4028.
[48] Gupte, A., Missoum, S., Sen, S., and Desai, J., 2007, "A Multidisciplinary Design Optimization Algorithm With Distributed Autonomous Subsystems," Proceedings of the 7th World Congress on Structural and Multidisciplinary Optimization, International Society for Structural and Multidisciplinary Optimization, pp. 481–491.

Downloaded from http://asmedigitalcollection.asme.org/computingengineering/article-pdf/24/9/091001/7347527/jcise_24_9_091001.pdf by guest on 07 September 2024